



Article

The CYP74 Gene Family in Watermelon: Genome-Wide Identification and Expression Profiling Under Hormonal Stress and Root-Knot Nematode Infection

Yong Zhou ^{1,2} , Yelan Guang ^{2,3}, Jingwen Li ^{2,3}, Fei Wang ¹, Golam Jalal Ahammed ⁴  and Youxin Yang ^{2,3,*} 

- ¹ Jiangxi Engineering Laboratory for the Development and Utilization of Agricultural Microbial Resources, College of Bioscience and Bioengineering, Jiangxi Agricultural University, Nanchang 330045, China; yongzhou@jxau.edu.cn (Y.Z.); wangfei179@163.com (F.W.)
- ² Key Laboratory of Crop Physiology, Ecology and Genetic Breeding, Ministry of Education, Jiangxi Agricultural University, Nanchang 330045, China; 15357167302@163.com (Y.G.); 18770911287@163.com (J.L.)
- ³ Jiangxi Key Laboratory for Postharvest Technology and Nondestructive Testing of Fruits & Vegetables, Collaborative Innovation Center of Post-Harvest Key Technology and Quality Safety of Fruits and Vegetables, College of Agronomy, Jiangxi Agricultural University, Nanchang 330045, China
- ⁴ College of Forestry, Henan University of Science and Technology, Luoyang 471023, China; ahammed@haust.edu.cn
- * Correspondence: yangyouxin@jxau.edu.cn

Received: 24 October 2019; Accepted: 9 December 2019; Published: 11 December 2019



Abstract: Allene oxide synthase (AOS) and hydroperoxide lyase (HPL), members of the CYP74 gene family, are branches of the oxylipin pathway and play vital roles in plant responses to a number of stresses. In this study, four *HPL* genes and one *AOS* gene were identified in the watermelon genome, which were clustered into three subfamilies (CYP74A, CYP74B and CYP74C). Sequence analysis revealed that most HPL and AOS proteins from various plants contain representative domains, including Helix-I region, Helix-K region (ExxR) and Heme-binding domain. A number of development-, stress-, and hormone-related *cis*-elements were found in the promoter regions of the *CIAOS* and *CIHPL* genes, and the detected *CIAOS* and *CIHPL* genes were differentially expressed in different tissues and fruit development stages, as well as in response to various hormones. In addition, red light could enhance the expression of *CIAOS* in root-knot nematode-infected leaves and roots of watermelon, implying that *CIAOS* might play a primary role in red light-induced resistance against root-knot nematodes. These findings lay a foundation for understanding the specific function of CYP74 genes in watermelon.

Keywords: watermelon; allene oxide synthase (AOS); hydroperoxide lyase (HPL); expression profile; root-knot nematode (RKN)

1. Introduction

Oxylipins are oxygenated derivatives from the oxidation of polyunsaturated fatty acids (PUFAs), which include jasmonic acid (JA) and its related compounds, as well as other molecules such as hydroxy-, oxo- or keto-fatty acids [1–3]. Oxylipin biosynthesis in plants originates from fatty acid hydroperoxides that are formed by the action of lipoxygenase (LOX), which is called the LOX pathway [4,5]. The fatty acid hydroperoxides then undergo several secondary conversions controlled by CYP74, which belongs to the superfamily of cytochrome P450 enzymes [4]. Allene oxide synthase (AOS), hydroperoxide lyase (HPL), and divinyl ether synthase (DES) are members of the CYP74 family, which can catalyze the

isomerization or dehydration of fatty acid hydroperoxides and require neither molecular oxygen nor NAD(P)H-dependent cytochrome P450-reductase [1,2,6].

CYP74 enzymes are broadly classified into four subfamilies (CYP74A, CYP74B, CYP74C, and CYP74D) based on their evolutionary heritage and relationship with the diversity of oxylipin structure [6]. AOS and DES members constitute the CYP74A and CYP74D subfamily, respectively, while CYP74B and CYP74C subfamilies contain enzymes with HPL activity [5,7]. In addition, AOS enzymes can be classified into three different types: The first two types can use either 13-hydroperoxide derivatives or 9-hydroperoxide derivatives as the substrate (13-AOS and 9-AOS, respectively), while the third type can use both of them (9/13-AOS) as the substrate [4,8]. Similarly, three types of HPL enzymes named as 13-HPL, 9-HPL, and 9/13-HPL were also reported in a number of plant species [9]. To date, AOS and HPL genes have been cloned and functionally characterized from a number of plant species, such as tomato (*Solanum lycopersicum* L. (Solanaceae)) [10,11], tobacco (*Nicotiana attenuate* Torr. ex S.Watson) [12], rice (*Oryza sativa* L.) [13,14], and barrel medic (*Medicago truncatula* Gaertn.) [15], whereas DES genes have been isolated in very few plants [16–20]. These findings reveal that plant CYP74 family genes are indispensable for oxylipin biosynthesis, and play important roles in plant growth and development, as well as in plant defense to various abiotic and biotic stresses.

Watermelon (*Citrullus lanatus* (Thunb.) Matsum. & Nakai) is an agricultural crop with high nutritional and economic values, but it is rather susceptible to various biotic and abiotic stresses during growth and development [21]. The root-knot nematodes (RKNs, *Meloidogyne incognita*) mainly infect the roots of host plants and increase susceptibility to other pathogenic diseases, and severely affect foliar growth and fruit yield of host plants [21,22]. In our previous report, red light (RL) exposure of watermelon leaves enhanced the systemic defense of the plant to RKN, which could be attributed to JA- and salicylic acid (SA)-dependent signaling, antioxidant activity, and redox homeostasis [23]. In this study, a systematic analysis of watermelon CYP74 genes was performed using bioinformatics methods, including genome-wide identification and analyses of phylogenetic relationships, protein and gene structures, and tissue expression patterns. In addition, we also determined the expression patterns of watermelon CYP74 genes under diverse hormonal stresses and RKN infection.

2. Materials and Methods

2.1. Identification of the CYP74 Genes in Watermelon Genome

The amino acid sequences of watermelon were downloaded from watermelon (97103) v1 genome database (<http://cucurbitgenomics.org/organism/1>). The conserved P450 domain (PF00067) was downloaded from the Pfam database (<http://pfam.xfam.org/>) and employed to searching for corresponding protein sequences with the HMMER software. In addition, the *Arabidopsis* HPL and AOS protein sequences were obtained from the Arabidopsis Information Resource (<https://www.arabidopsis.org/>) according to previous reports [24–26]. Then, these sequences were used as queries to perform a BLASTP search against the protein sequences of watermelon. All identified CYP74 proteins were submitted to InterPro (<http://www.ebi.ac.uk/interpro/>) and NCBI CDD database (<https://www.ncbi.nlm.nih.gov/Structure/cdd/wrpsb.cgi/>) to check whether the proteins harbored the conserved P450 domain.

2.2. Protein Properties, Chromosomal Locations, and Promoter Analysis

The theoretical isoelectric point (pI), molecular weight (MW), and grand average of hydropathicity (GRAVY) of watermelon CYP74 proteins were determined using ProtParam (<https://web.expasy.org/protparam/>). The subcellular localization of the watermelon CYP74 proteins was predicted using ProtComp 9.0 (<http://linux1.softberry.com/>). The chromosomal locations of watermelon CYP74 genes were obtained from watermelon (97103) v1 genome database, and the segmental and tandem duplications were checked based on the methodology in a previous study [27]. To identify the putative

cis-acting regulatory elements of the promoter regions of watermelon CYP74 genes, the 1,500-bp sequences upstream the start codon of watermelon CYP74 genes were retrieved and analyzed using PlantCARE tool (<http://bioinformatics.psb.ugent.be/webtools/plantcare/html/>).

2.3. Phylogenesis, Conserved Motif, and Gene Structure Analyses

CYP74 enzyme family proteins from different plant species used in this study are listed in Table S1. Multiple sequence alignments of these full-length CYP74 protein sequences were performed using MAFFT [28], and the alignments were visualized using the GeneDoc software. Then, the alignments were employed to create an unrooted phylogenetic tree by the MEGA 7.0 software using the neighbor-joining (NJ) method with 1000 bootstrap replicates and the pairwise deletion option. The conserved motifs of CYP74 proteins were defined using the MEME online tool (<http://meme-suite.org/>) with default parameters, and the motif diagrams were drawn using the TBtools software [29]. For the gene structure analysis, the genomic DNA (gDNA) sequence and corresponding coding sequence (CDS) of each CYP74 gene were aligned and the structure diagrams were drawn on GSDS (<http://gsds.cbi.pku.edu.cn/>).

2.4. Expression Profiles of Watermelon CYP74 Genes Based on RNA-seq Data

To study the expression profiles of watermelon CYP74 genes during fruit development, the raw RNA-seq data of the flesh and rind at four pivotal stages of fruit development were obtained from a previous report [30]. To assess the expression profiles of watermelon CYP74 genes during RKN infection, the raw RNA-seq data under the treatments of CK (white light and water solution), RL (red light and water solution), RKN (white light and *M. incognita* infection), and RR (red light and *M. incognita* infection) were obtained and analyzed [23]. The expression levels of watermelon CYP74 genes were retrieved and estimated with FPKM (fragments per kilobase of exon per million fragments mapped) values as previously described [21]. The differentially expressed genes were identified with a cutoff of $|\text{fold change}| \geq 1.5$.

2.5. Plant Materials and Growth Conditions

The seedlings of watermelon (*Citrullus lanatus* L. cv. Xinong 8) were grown in a greenhouse under the conditions of light intensity of $200 \mu\text{mol}\cdot\text{m}^{-2}\cdot\text{s}^{-1}$ (12 h/12 h), and 25 °C/19 °C (12 h/12 h). Two-month-old seedlings were harvested for collecting the tissues including the roots, stems, stem apices, leaves, fruits, and flowers. Hormonal treatments, including 100 μM methyl jasmonate (MeJA), 500 μM ethylene (ET), and 1 mM salicylic acid (SA), were carried out according to our previous study [31], and the roots or leaves before and after different hormonal treatments were collected. All samples were immediately frozen in liquid nitrogen and stored at -80°C for RNA extraction.

2.6. Quantitative Reverse Transcriptase-Polymerase Chain Reaction (qRT-PCR) Analysis

The total RNA of all samples was extracted with the total RNA Miniprep Kit (Axygen Biosciences, Union City, CA, USA) following the manufacturers' recommendations. The RNA was reverse transcribed using the ReverTra Ace qPCR-RT Kit (TOYOBO, Osaka, Japan). qRT-PCR was performed on the iCycler iQTM Real-time PCR Detection System (Bio-Rad, Hercules, CA, USA) in three replicates. The PCR was performed as follows: 3 min at 95 °C, followed by 40 cycles of 30 s at 95 °C, 30 s at 58 °C, and 1 min at 72 °C. Watermelon β -actin gene (Cl007792) was used as an internal control, and the value of relative expression was analyzed using the method described in a previous study [32]. The gene-specific primers are listed in Table S2.

3. Results

3.1. Genome-Wide Identification and Gene Duplication of the CYP74 Genes in Watermelon

Four HPL genes and one AOS gene were identified in the watermelon genome and were designated as *CIHPL1*–*CIHPL4* and *CIAOS* based on their chromosome locations (Table 1). Similar to the case in *Arabidopsis*, divinyl-ether synthase (DES) was not identified in the watermelon genome [33]. The five watermelon CYP74 genes were irregularly distributed on two chromosomes of the watermelon genome. The CDS and gDNA lengths of watermelon CYP74 genes were 573–1599 bp and 1526–3964 bp, respectively. The number of amino acids of watermelon CYP74 proteins varied from 190 (*CIHPL1*) to 532 (*CIAOS*), and the associated theoretical pI, MW, and GRAVY values were 5.55–9.69, 21.54–60.18 kDa, and from −0.285 to −0.132, respectively. Subcellular prediction results showed that all of the watermelon CYP74 proteins were localized in the chloroplast, with the exception of *CIHPL3*, which was a cytoplasmic protein.

Table 1. Accession members and characteristics of the CYP74 genes in watermelon.

Gene	Gene ID	Genomic Position	gDNA (bp)	CDS (bp)	Protein (aa)	pI	MW (kDa)	GRAVY	Subcellular Prediction
<i>CIHPL1</i>	Cla007649	Chr2: 1075–3042 (+)	1968	573	190	9.69	21.54	−0.217	Chloroplast
<i>CIHPL2</i>	Cla007650	Chr2: 7515–11478 (+)	3964	1008	335	5.55	38.07	−0.170	Chloroplast
<i>CIHPL3</i>	Cla015969	Chr2: 5586383–5587923 (−)	1541	1446	481	8.10	54.14	−0.160	Cytoplasmic
<i>CIHPL4</i>	Cla015970	Chr2: 5597014–5598539 (−)	1526	1443	480	7.62	54.20	−0.132	Chloroplast
<i>CIAOS</i>	Cla022526	Chr8: 24373048–24374646 (+)	1599	1599	532	9.02	60.18	−0.285	Chloroplast

Among these genes, all *CIHPL* genes were located in chromosome 2, while *CIAOS* was located in chromosome 8 (Table 1 and Figure 1). According to the criteria in a previous report [34], one segmental duplication event (*CIHPL3* and *CIAOS*) was identified, while two pairs of genes (*CIHPL1* and *CIHPL2*; *CIHPL3* and *CIHPL4*), were generated from tandem gene duplications (Figure 1).

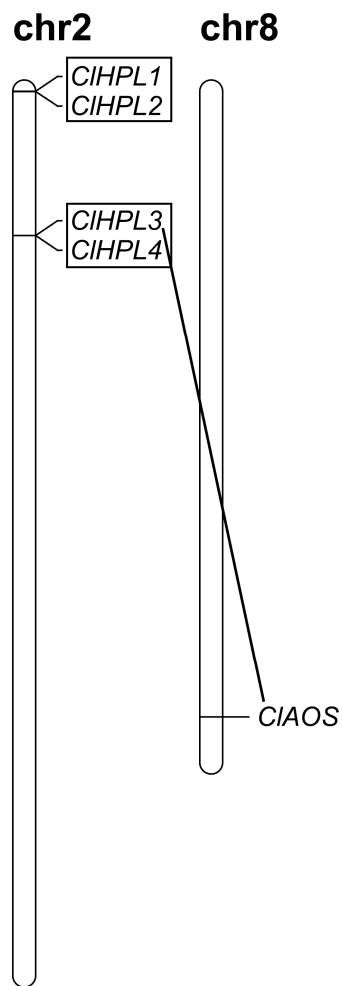


Figure 1. Chromosomal locations of *CIAOS* and *CIHPL* genes in watermelon. The segmental and tandem duplicated genes are connected by black lines and boxed, respectively.

3.2. Phylogenetic Relationships of the CYP74 Proteins in Watermelon and Other Plant Species

To reveal the phylogenetic relationships of watermelon *CYP74* genes with those from other plants, a neighbor-joining (NJ) tree of watermelon *CYP74* proteins and the corresponding orthologs from cucumber (*Cucumis sativus* L.) [35], common bean (*Phaseolus vulgaris* L.) [36], barrel medic (*M. truncatula*) [15], and *Arabidopsis* were generated. As a result, these *CYP74* proteins were clustered into three subfamilies (*CYP74A*, *CYP74B*, and *CYP74C*) (Figure 2). *DES*, which belongs to the *CYP74D* subfamily of the cytochrome P450 superfamily, was not identified in these plant species [2,6]. *CIAOS* was grouped with other plant AOS proteins into the *CYP74A* subfamily, which was distinct from HPLs (Figure 2). HPLs from these plants were grouped into two subfamilies, *CYP74B* and *CYP74C*. *CIHPL1* and *CIHPL2* were clustered together with other 13-HPL sequences in the *CYP74B* subfamily, while *CIHPL3* and *CIHPL4* were clustered together with other 9-HPL and 9/13-HPL sequences in the *CYP74C* subfamily (Figure 2).

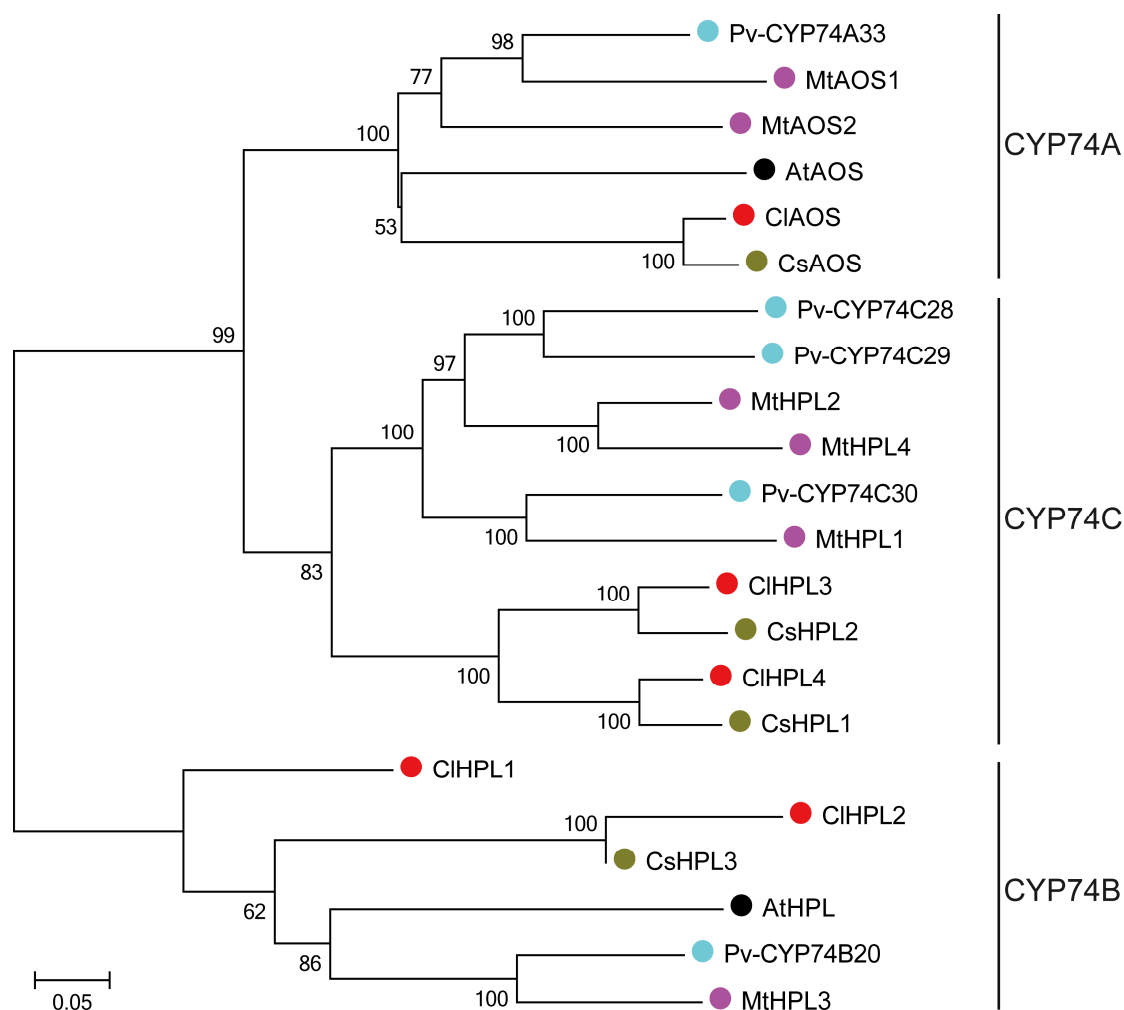


Figure 2. Phylogenetic analysis of CYP74 proteins among watermelon and other plant species. The numbers at the nodes represent bootstrap percentage values based on 1000 replications.

3.3. Characterization and Conserved Motif Analysis of CYP74 Proteins in Watermelon and Other Plant Species

Multiple sequence alignment results revealed that three representative domains, including Helix-I region (FNxxGGxKxxxP), Helix-K region (ExxR), and Heme-binding domain (PxxxNKQCxGKD), were highly conserved among all the HPL and AOS proteins from watermelon and other plants, with the exception of CIHPL1 (Figure 3). To explore the conserved motifs within CYP74 proteins, the MEME tool was used to discover the conserved motifs of CYP74 proteins from *Arabidopsis*, cucumber, common bean, *Medicago truncatula*, and watermelon. A total of 10 distinct motifs were identified, all of which were present in all CYP74A and CYP74C proteins (Figure 4 and Table S3). However, CYP74B proteins were lacked of certain motifs. For example, CsHPL3, Pv-CYP74B20 and MtHPL3 were lacked of motif 9, while motifs 4 and 5 were absent in AtHPL (Figure 4).

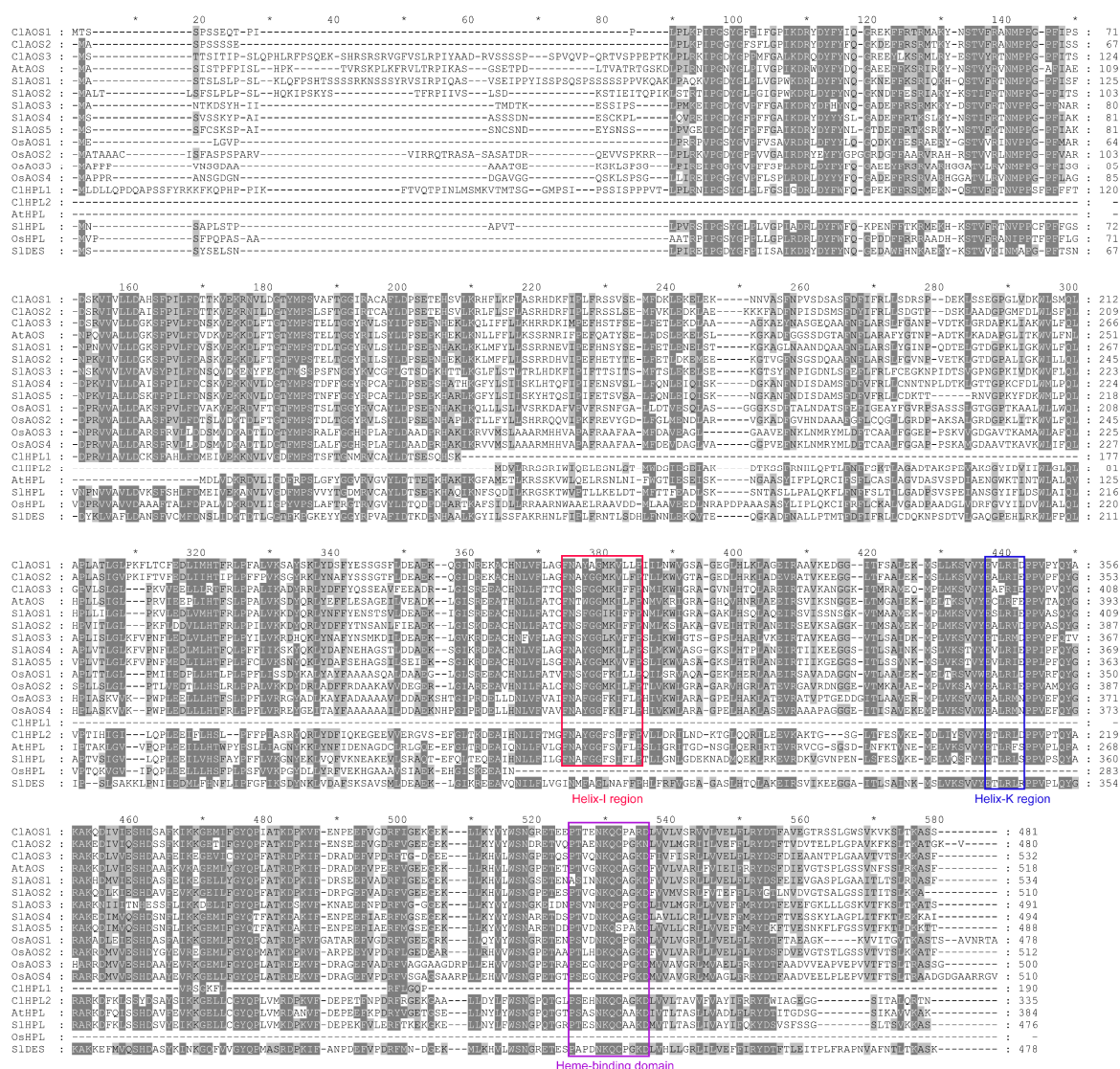


Figure 3. Sequence alignment of CYP74 protein sequences from watermelon and other plant species. The three boxes indicate the Helix-I region (FNxxGGxKxxxP), Helix-K region (ExxR), and Heme-binding domain (PxxxNKLQCxGKD), respectively. At, *Arabidopsis thaliana*; Sl, *Solanum lycopersicum*; Os, *Oryza sativa*; Cl, *Citrullus lanatus*.

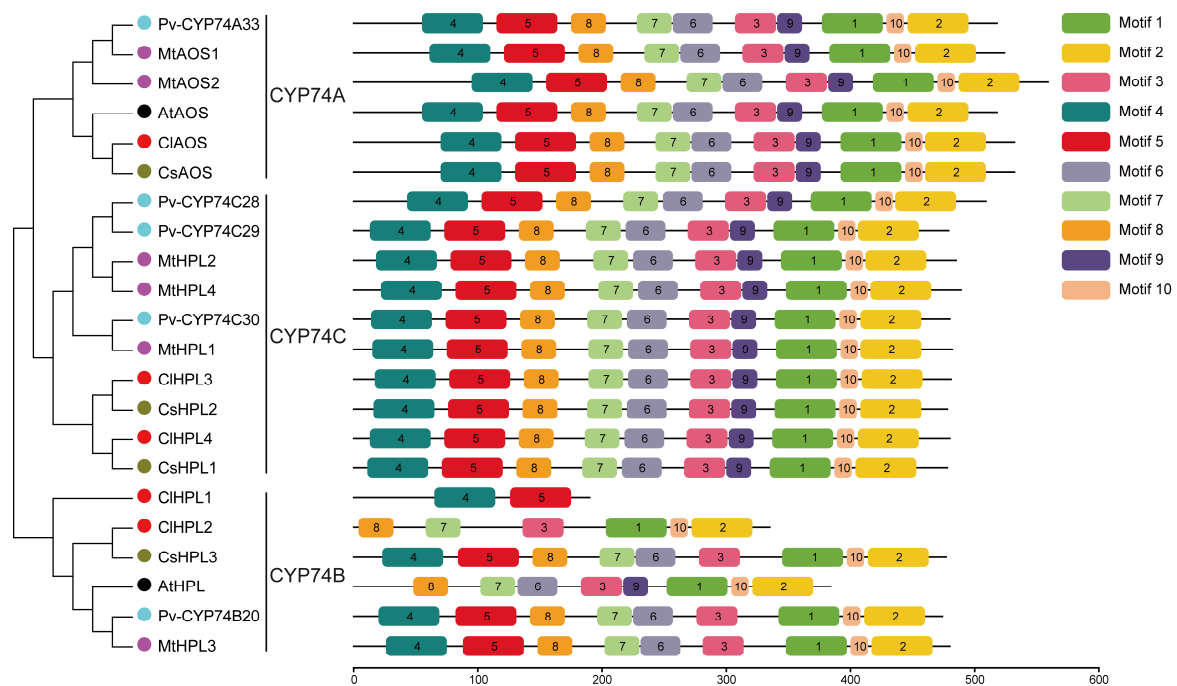


Figure 4. Conserved domain compositions of CYP74 proteins in watermelon and other plant species according to phylogenetic analysis. At, *Arabidopsis thaliana*; Cs, *Cucumis sativus*; Pv, *Phaseolus vulgaris*; Mt, *Medicago truncatula*; Cl, *Citrullus lanatus*.

3.4. Structural Analysis of CYP74 Genes in Watermelon and Other Plant Species

The structures of CYP74 genes from watermelon and other plant species were determined by alignment of the CDS sequences to the gDNA sequences. As shown in Figure 5, the intron numbers of these CYP74 genes varied from 0 to 2, and all CYP74A members were intron-less, whereas the majority of CYP74B and CYP74C subfamily genes harbored one to two introns, with the exception of *MtHPL1*, which also contained no intron (Figure 5).

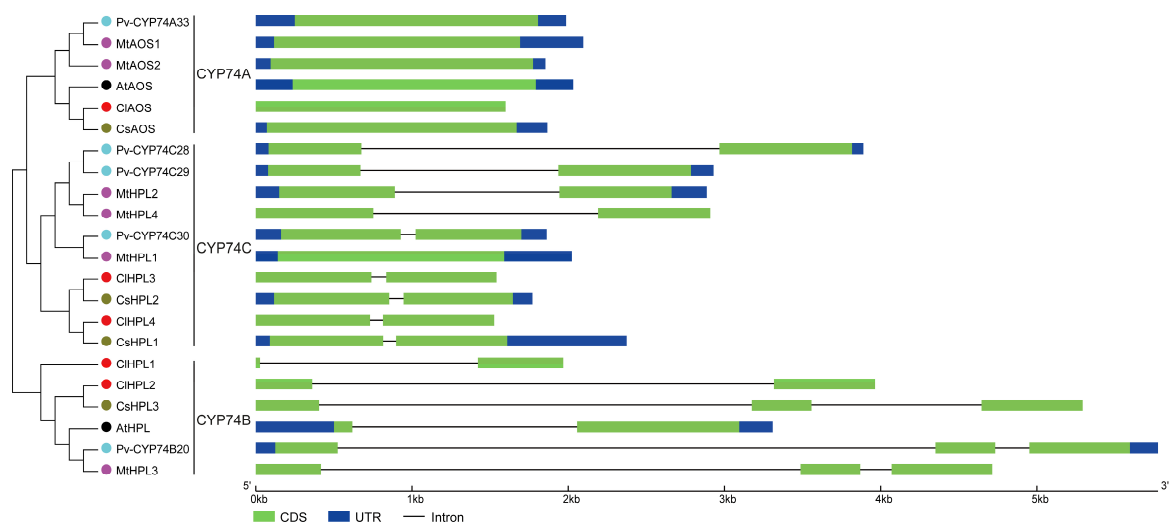


Figure 5. Gene structures of CYP74 genes in watermelon and other plant species according to phylogenetic analysis. The blue boxes, green boxes, and black lines indicate UTRs, CDSs, and introns, respectively. At, *Arabidopsis thaliana*; Cs, *Cucumis sativus*; Pv, *Phaseolus vulgaris*; Mt, *Medicago truncatula*; Cl, *Citrullus lanatus*.

3.5. Cis-Element Analysis of Watermelon CYP74 Genes

To assess the possible transcriptional regulation of watermelon CYP74 genes, 1500-bp sequences upstream of the translation start site of *CIHPL* and *CIAOS* genes were scanned by using PlantCARE. The results indicated the presence of 14 types of development-, stress-, and hormone-related *cis*-elements in the promoter regions of the *CIHPL* and *CIAOS* genes (Figure 6). Only two kinds of *cis*-elements were found to be related to development, including GCN4 motif and O2-site, which were involved in endosperm expression and zein metabolism regulation, respectively (Figure 6). The two development-related *cis*-elements were only present in the promoters of *CIHPL1*, *CIHPL3*, and *CIHPL4*. Several stress-related *cis*-elements, such as LTR (low-temperature responsiveness element), TC-rich repeats (defense and stress responsiveness element), WUN-motif (wound-responsive element), W-box (WRKY binding site involved in abiotic stress and defense response), and ARE (anaerobic induction element), were identified in the promoters of *CIHPL* and *CIAOS* genes (Figure 6). Notably, the ARE element was much more abundant than other stress-related *cis*-elements, especially in the promoters of *CIHPL2* and *CIHPL4*. Seven kinds of hormone-related *cis*-elements were found in the *CIHPL* and *CIAOS* promoters (Figure 6). For example, one or more ethylene responsive elements (ERE) were identified in the promoters of *CIHPL* and *CIAOS* genes. Additionally, the *cis*-element related to MeJA (CGTCA-motif) was found in *CIHPL2-4* and *CIAOS* but not in *CIHPL1*, and the *cis*-element associated with auxin (TGA-element) was found in *CIHPL4*, but not in other genes (Figure 6). There were abscisic acid (ABA) responsive elements (ABRE) in the promoters of *CIHPL4* and *CIAOS*, and gibberellin-responsive elements (GARE-motif, P-box, and TATC-box) in the promoters of *CIHPL2-4* (Figure 6). These results implied that the watermelon CYP74 genes might be involved in plant development and responses to hormone and various stresses.

	Development		Stress					Hormone						
	GCN4_motif	O2-site	LTR	TC-rich repeats	WUN-motif	W-box	ARE	CGTCA-motif	ABRE	GARE-motif	ERE	P-box	TATC-box	TGA-element
<i>CIHPL1</i>	1	1		1							1			
<i>CIHPL2</i>						1	3	1			2	1	1	
<i>CIHPL3</i>	1		1				1	1		1	3			
<i>CIHPL4</i>		1		1	1	1	4	2	1		3	1		2
<i>CIAOS</i>			1		2		2	1	1		2			

Figure 6. Analysis of development-, hormone-, and stress-related *cis*-elements in the promoter regions of watermelon CYP74 genes. *Cis*-elements are shown by different colors and numbers in the grids.

3.6. Expression Analysis of Watermelon CYP74 Genes in Different Tissues and During Fruit Development

To investigate the tissue-specific expression profiles of watermelon CYP74 genes, the expression levels of *CIHPL1*, *CIHPL2*, and *CIAOS* were determined in five tissues and organs by qRT-PCR, including the leaf, root, stem, flower, and fruit. *CIHPL1* and *CIHPL2* showed similar expression patterns, with the highest expression in fruit, moderate expression in leaf, and relatively lower expression in other tissues, particularly in root (Figure 7A). *CIAOS* was also highly expressed in fruit and flower and had weak expression in other tissues (Figure 7A).

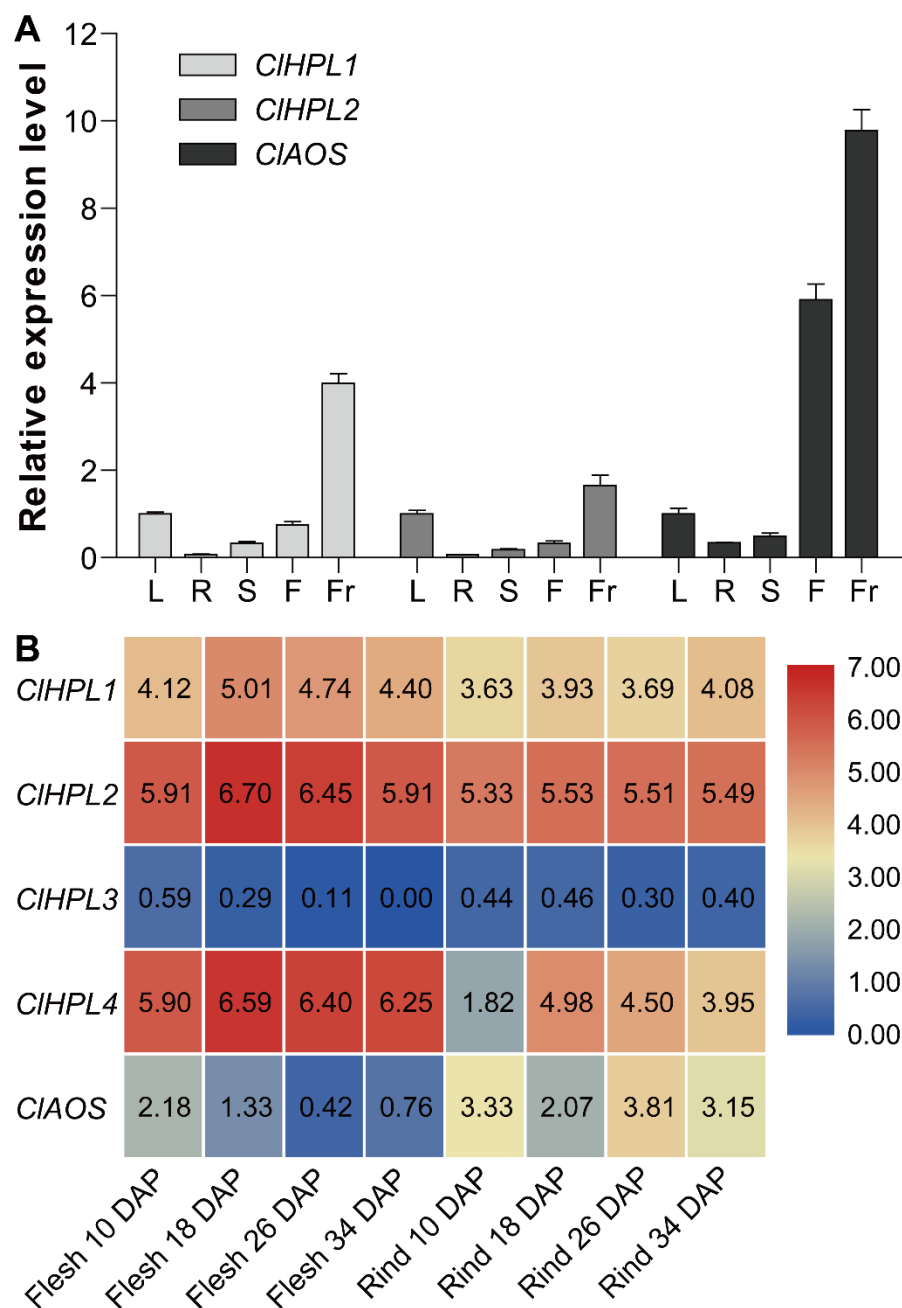


Figure 7. Expression profiles of watermelon *CYP74* genes in different tissues and during fruit development in watermelon. (A) qRT-PCR analysis. L, leaf; R, root; S, stem; F, flower; Fr, fruit. (B) The expression levels are indicated as log2-based FPKM+1 values. DAP, days after pollination.

To study the potential role of watermelon *CYP74* genes in fruit development, their expression in the flesh and rind was determined at different developmental stages based on previously published transcriptome data [30]. *CIHPL1* and *CIHPL2* were highly expressed during the development of flesh and rind, while *CIHPL3* was weakly expressed at all stages of flesh and rind development (Figure 7B). Both *CIHPL4* and *CIAOS* showed significant transcriptional changes at all stages of flesh and rind development (Figure 7B). These results indicated that watermelon *CYP74* genes might be involved in fruit development.

3.7. Expression Analysis of Watermelon CYP74 Genes Under Hormonal Treatments

To study the effects of different hormones on the expression of watermelon CYP74 genes, the expression profiles of the *CIHPL* and *CIAOS* genes in the leaf and root were analyzed under JA, SA, and ET treatments. The results showed that all these genes were dramatically up-regulated in response to the three hormones (Figure 8). *CIHPL1* and *CIHPL2* had similar expression patterns under JA, SA, and ET treatments, with the expression levels gradually increasing at the earlier time points and peaking at 9 h, and then decreasing sharply at 24 h (Figure 8). Under JA treatment, the expression of *CIHPL3* and *CIAOS* was obviously up-regulated in both the leaf and root, but the expression of *CIAOS* was much higher than that of *CIHPL3* and displayed a declining trend at 9 h and 24 h (Figures 7B and 8A). Under SA and ET treatments, the expression levels of *CIHPL3* and *CIAOS* also increased observably at earlier time points (1 h and 3 h) and then decreased gradually at 9 h and 24 h (Figures 7D and 8C). These results indicated the possible functions of these genes in mediating various hormone signaling pathways in watermelon.

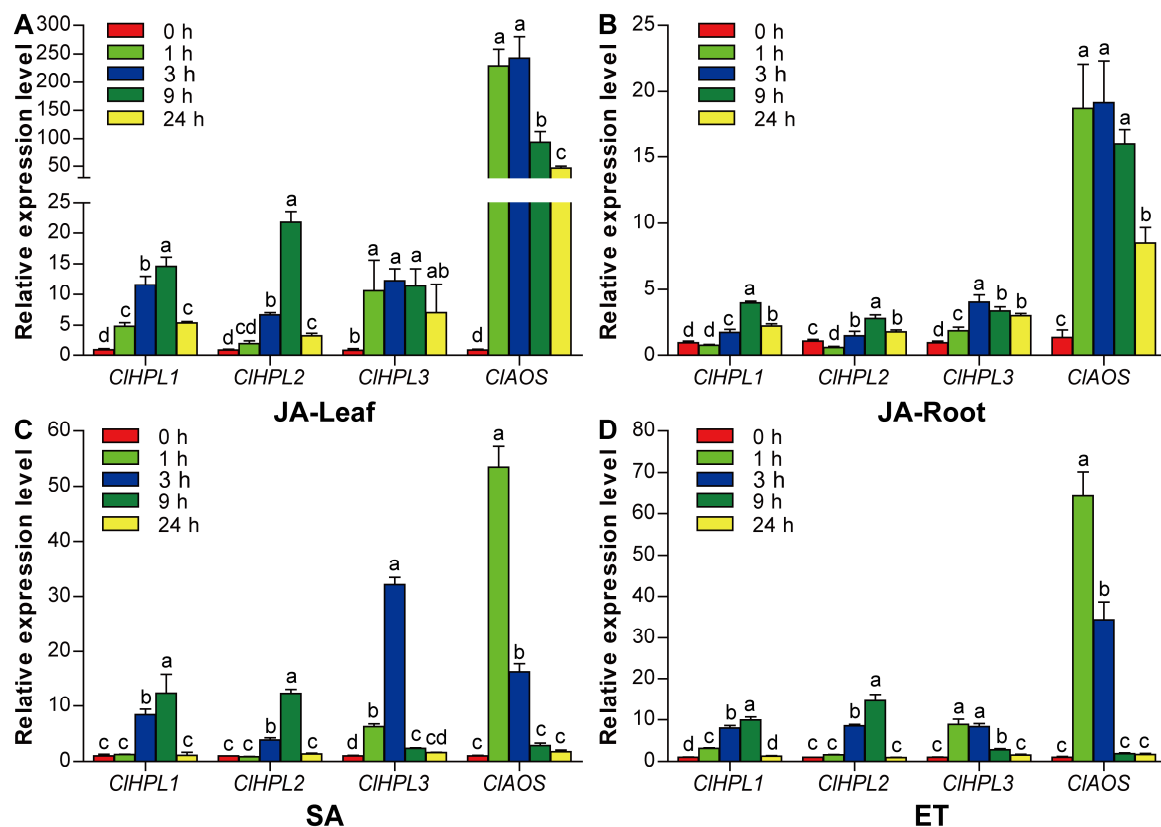


Figure 8. qRT-PCR analysis of the expression profiles of watermelon CYP74 genes in leaves and roots under jasmonic acid (JA), salicylic acid (SA), and ethylene (ET) treatments. The leaves (A,C,D) and roots (B) of the watermelon seedlings were used to examine the expression levels of the *CIHPL* and *CIAOS* genes using qRT-PCR at different time points (0, 1, 3, 9 and 24 h). The differences between different treatment times are indicated by different letters above the bars (Tukey's multiple range tests, $p < 0.05$).

3.8. Expression Patterns of Watermelon CYP74 Genes in Response to Root-Knot Nematode Infection

To assess the role of watermelon CYP74 genes during RKN infection and development, we examined the expression of *CIAOS* and *CIHPL* genes under the treatments of CK, RKN, RL, and RR using previous transcriptome data [23]. In leaves, both *CIHPL1* and *CIHPL2* were down-regulated by RKN treatment relative to CK, while their expression levels were unchanged under the treatments of RL and RR (Figure 9). In leaves, RR treatment observably up-regulated four watermelon CYP74 genes

(*CIHPL1*, *CIHPL2*, *CIHPL3*, and *CIAOS*) compared with RKN treatment (Figure 9). In roots, *CIAOS* was down-regulated by RL treatment compared with CK, and its expression was up-regulated under RR treatment compared with RKN treatment (Figure 9).

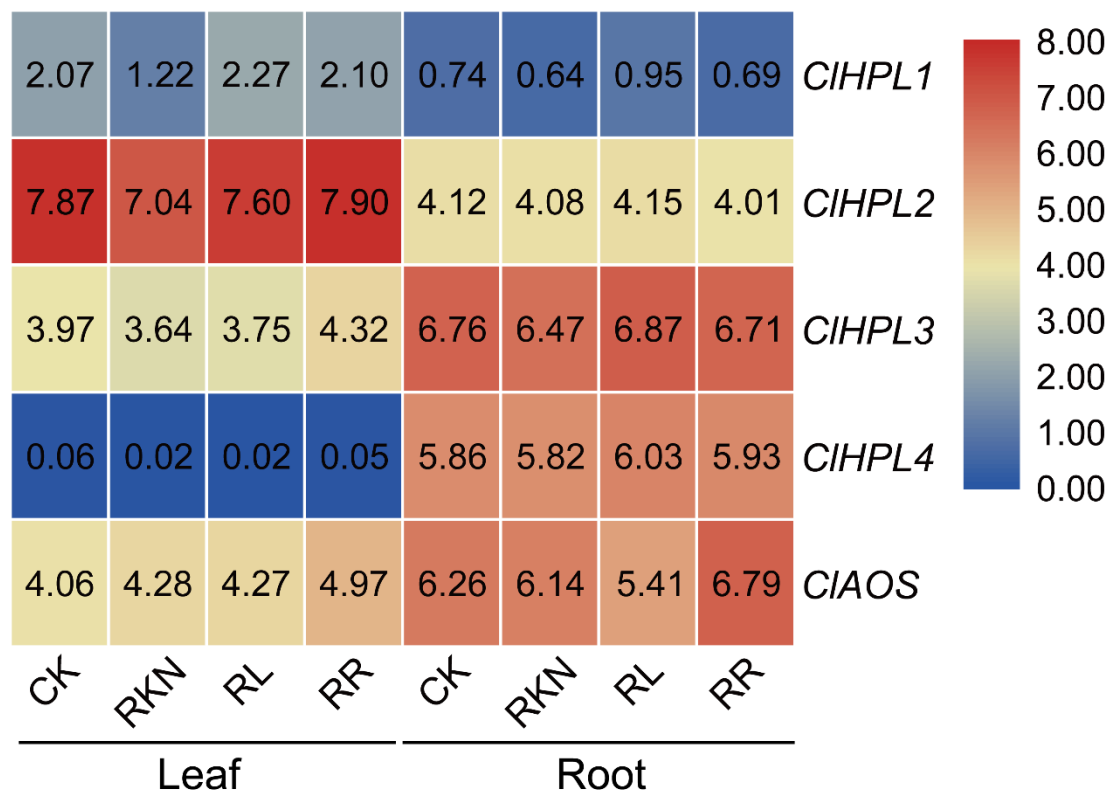


Figure 9. Expression profiles of watermelon CYP74 genes in leaves and roots with nematode inoculation under the treatments of CK (white light and water solution), RL (red light and water solution), RKN (white light and *M. incognita* infection), and RR (red light and *M. incognita* infection). The expression levels are indicated as log2-based FPKM+1 values.

4. Discussion

In this study, genome-wide identification of the CYP74 gene family was performed in watermelon. A total of four HPL genes and one AOS gene were identified in the watermelon genome, while no DES genes were identified (Table 1). In previous reports, only a single gene was found to encode AOS in various plants, such as *Arabidopsis* [24,25], cucumber [9,35], common bean [36], grapevine [37,38], *Brassica* species [39], and the numbers of HPL genes in these plants were 1, 3, 4, 4, 1, and 1, respectively. In addition, rice harbors three OsHPL genes and two OsAOS genes [13,40–42], and *M. truncatula* has four MtHPL genes and two MtAOS genes [15]. However, no DES genes were identified in these plants. In the present study, AOS was also encoded by a single gene, but the HPL genes existed in multiple copies. According to the criteria in a previous report [27], two tandem duplication events and one segmental duplication event were identified (Figure 1). A previous study showed that a single amino acid exchange leads to the conversion of an AOS to an HPL [43]. These results suggest that the CYP74 genes, especially HPL genes, have undergone significant expansion during evolution in watermelon.

The phylogenetic tree revealed that HPL and AOS proteins from *Arabidopsis*, cucumber, common bean, *Medicago truncatula*, and watermelon can be grouped into three subfamilies, which were named CYP74A, CYP74B, and CYP74C, as defined by cytochrome P450 nomenclature (Figure 2). Amongst them, the CYP74A subfamily contains only AOS sequences. HPLs in these plants were grouped into two subfamilies depending on their substrate specificity, 13-HPLs (CYP74B) and 9-/13-HPLs (CYP74C), which was similar to the results in previous studies [6,13,41]. Amino acid alignment

clearly indicated that three representative domains, Helix-I region, Helix-K region, and Heme-binding domain, were present in nearly all of the HPL and AOS proteins in various plants (Figure 3), suggesting that these domains are essential for the functions of the CYP74 enzymes in plants. We further detected the conserved motifs by MEME tool. The results showed that all CYP74A and CYP74C proteins possessed all 10 conserved motifs, while CYP74B proteins lacked certain motifs (Figure 4). Indeed, the phylogenetic analysis showed that CYP74C proteins from various plants were more closely related to CYP74A than to CYP74B proteins (Figure 2), implying that CYP74A and CYP74C subfamily members were highly conserved during evolution. Moreover, the results of gene structure analysis also confirmed the reliability of the phylogenetic tree. For example, some genes in the same group exhibited the same number of introns with CDS lengths highly similar to each other, such as *Pv-CYP74C28/Pv-CYP74C29*, *MtHPL2/MtHPL4*, and *CIHPL3/CsHPL2/CIHPL4/CsHPL1* in the CYP74B subfamily, and *Pv-CYP74B20/MtHPL3* in the CYP74C subfamily, implying their similar functions in plants (Figure 5).

To functionally characterize the CYP74 genes, we first assessed the expression profiles of three genes (*CIHPL1*, *CIHPL2* and *CIAOS*) in different tissues by qRT-PCR. As a result, the three genes were found to be highly expressed in fruit, especially *CIAOS* (Figure 7A). Similarly, *VvAOS* was shown to have the highest expression in the pulp of mature berries [37]. In addition, the three genes also displayed relatively higher expression levels in flower and leaf. In grapevine, *VvHPL2* had much higher expression in leaf and flower than in other tissues [38]. The transcriptome data were used to assess the expression of CYP74 genes during fruit development. Although the expression of *CIAOS* and *CIHPL* genes could be detected during the development of flesh and rind, there were obvious variations in their expression in developing flesh and rind (Figure 7B), which is consistent with the expression patterns of their homologous genes reported in other species, such as tomato [11], cucumber [9], and grapevine [38].

Oxylipins are a class of secondary metabolites derived from the LOX pathway, and products of this pathway are involved in responses to various biotic and abiotic stresses of plants, including wound healing, drought, pathogen attack, pest resistance, and hormone signaling [2,6,44,45]. In this study, a number of stress- and hormone-related *cis*-elements were found in the promoter regions of *CIAOS* and *CIHPL* genes (Figure 6), suggesting that they may play certain roles in response to various stresses and hormones. For example, one and two WUN-motifs were respectively present in promoters of *CIHPL4* and *CIAOS*, implying that these two genes may be involved in wound healing. In rice, the expression of *OsHPL3* was found to be induced by wounding [40]. In *M. truncatula*, wounding was found to trigger an early and strong up-regulation of *AOS* and *HPL* genes in the aerial tissues accompanied by the biosynthesis of more jasmonate [15]. Besides, spatial and temporal dynamics of jasmonate burst upon leaf wounding were also reported in *Arabidopsis* [46]. In addition, *AOS* and *HPL* genes were also found to be up-regulated in response to various biotic stresses. For example, wounding or inoculation with nonpathogenic *Alternaria alternata* could rapidly lead to the transcript accumulation of the *HPL* and *AOS* genes in rough lemon [47]. In this study, *CIAOS* was up-regulated under RR treatment compared with RKN treatment in both leaves and roots (Figure 9), suggesting its important role in RL-induced systemic resistance against RKN infection. *AOS* is a key enzyme for the biosynthesis of jasmonate, which plays vital roles in responses to various biotic stresses [48–50]. In addition, *CIAOS* possessed many hormone-related *cis*-elements (Figure 6) and exhibited more dramatically up-regulated expression in response to JA, SA, and ET than other detected *CIHPL* genes (Figure 8). Our previous report has revealed that RL-induced systemic resistance against RKN infection could be attributed to the accumulation of JA and SA [23]. JA, SA, and ET are vital components in plant defense against RKN infection in various plants [51–55]. Further studies need to be carried out to reveal the roles of *CIAOS* and *CIHPL* genes in regulating responses to various biotic and abiotic stresses of watermelon.

5. Conclusions

In summary, we identified five *CYP74* genes in the watermelon genome, including four *CIHPLs* and one *CIAOS*, which were classified into three distinct subfamilies (*CYP74A*, *CYP74B*, and *CYP74C*). We also analyzed their phylogenetic relationships, protein and gene structures, *cis*-elements, tissue expression patterns, and responses to various hormones, nematodes infection, and red light exposure. *CIAOS* showed more significant variations in expression than other *CYP74* genes under red light and nematode infection, indicating that the jasmonate biosynthesis from the AOS pathway plays a vital role in nematode resistance. Our results may lay a foundation for understanding the roles of *CYP74* genes and provide important information for genetic engineering of watermelon.

Supplementary Materials: The following are available online at <http://www.mdpi.com/2073-4395/9/12/872/s1>, Table S1: *CYP74* enzyme family proteins from different plant species used in this study, Table S2: Primers sequences used in qRT-PCR, Table S3: Sequences and lengths of motifs among plant *CYP74* proteins.

Author Contributions: Data curation, Y.Z., Y.G., J.L., and Y.Y.; formal analysis, Y.G. and J.L.; funding acquisition, Y.Z. and Y.Y.; investigation, Y.Z.; methodology, Y.G., F.W., and Y.Y.; resources, F.W. and Y.Y.; software, J.L.; writing—original draft, Y.Z.; writing—review and editing, Y.Z., G.J.A., and Y.Y.; visualization, Y.Z., G.J.A., and Y.Y.

Funding: This research was funded by the National Natural Science Foundation of China (31560572), the Natural Science Foundation of Jiangxi Province, China (20171BAB214030), and the Foundation of Jiangxi Educational Committee (GJJ160393 and GJJ180172).

Conflicts of Interest: The authors declare no conflict of interest.

References

- Mosblech, A.; Feussner, I.; Heilmann, I. Oxylipins: Structurally diverse metabolites from fatty acid oxidation. *Plant Physiol. Biochem.* **2009**, *47*, 511–517. [CrossRef] [PubMed]
- Wasternack, C.; Feussner, I. The oxylipin pathways: Biochemistry and function. *Annu. Rev. Plant Biol.* **2018**, *69*, 363–386. [CrossRef] [PubMed]
- Andreou, A.; Brodhun, F.; Feussner, I. Biosynthesis of oxylipins in non-mammals. *Prog. Lipid Res.* **2009**, *48*, 148–170. [CrossRef] [PubMed]
- Stumpe, M.; Feussner, I. Formation of oxylipins by *CYP74* enzymes. *Phytochem. Rev.* **2006**, *5*, 347–357. [CrossRef]
- Feussner, I.; Wasternack, C. The lipoxygenase pathway. *Annu. Rev. Plant Biol.* **2002**, *53*, 275–297. [CrossRef]
- Howe, G.A.; Schilmiller, A.L. Oxylipin metabolism in response to stress. *Curr. Opin. Plant Biol.* **2002**, *5*, 230–236. [CrossRef]
- Grechkin, A.N. Hydroperoxide lyase and divinyl ether synthase. *Prostaglandins Other Lipid Mediat.* **2002**, *68–69*, 457–470. [CrossRef]
- Gorina, S.S.; Mukhitova, F.K.; Ilyina, T.M.; Toporkova, Y.Y.; Grechkin, A.N. Detection of unprecedented allene oxide synthase member of *CYP74B* subfamily: *CYP74B33* of carrot (*Daucus carota*). *Biochim. Biophys. Acta Mol. Cell Biol. Lipids* **2019**, *1864*, 1580–1590. [CrossRef]
- Wan, X.H.; Chen, S.X.; Wang, C.Y.; Zhang, R.R.; Cheng, S.Q.; Meng, H.W.; Shen, X.Q. Isolation, expression, and characterization of a hydroperoxide lyase gene from cucumber. *Int. J. Mol. Sci.* **2013**, *14*, 22082–22101. [CrossRef]
- Froehlich, J.E.; Itoh, A.; Howe, G.A. Tomato allene oxide synthase and fatty acid hydroperoxide lyase, two cytochrome P450s involved in oxylipin metabolism, are targeted to different membranes of chloroplast envelope. *Plant Physiol.* **2001**, *125*, 306–317. [CrossRef]
- Howe, G.A.; Lee, G.I.; Itoh, A.; Li, L.; DeRocher, A.E. Cytochrome P450-dependent metabolism of oxylipins in tomato. Cloning and expression of allene oxide synthase and fatty acid hydroperoxide lyase. *Plant Physiol.* **2000**, *123*, 711–724. [CrossRef] [PubMed]
- Halitschke, R.; Ziegler, J.; Keinänen, M.; Baldwin, I.T. Silencing of hydroperoxide lyase and allene oxide synthase reveals substrate and defense signaling crosstalk in *Nicotiana attenuata*. *Plant J.* **2004**, *40*, 35–46. [CrossRef] [PubMed]

13. Liu, X.; Li, F.; Tang, J.; Wang, W.; Zhang, F.; Wang, G.; Chu, J.; Yan, C.; Wang, T.; Chu, C.; et al. Activation of the jasmonic acid pathway by depletion of the hydroperoxide lyase OsHPL3 reveals crosstalk between the HPL and AOS branches of the oxylipin pathway in rice. *PLoS ONE* **2012**, *7*, e50089. [[CrossRef](#)] [[PubMed](#)]
14. Kuroda, H.; Oshima, T.; Kaneda, H.; Takashio, M. Identification and functional analyses of two cDNAs that encode fatty acid 9-/13-hydroperoxide lyase (CYP74C) in rice. *Biosci. Biotechnol. Biochem.* **2005**, *69*, 1545–1554. [[CrossRef](#)] [[PubMed](#)]
15. De Domenico, S.; Taurino, M.; Gallo, A.; Poltronieri, P.; Pastor, V.; Flors, V.; Santino, A. Oxylipin dynamics in *Medicago truncatula* in response to salt and wounding stresses. *Physiol. Plant.* **2019**, *165*, 198–208. [[CrossRef](#)] [[PubMed](#)]
16. Stumpe, M.; Kandzia, R.; Gobel, C.; Rosahl, S.; Feussner, I. A pathogen-inducible divinyl ether synthase (CYP74D) from elicitor-treated potato suspension cells. *FEBS Lett.* **2001**, *507*, 371–376. [[CrossRef](#)]
17. Itoh, A.; Howe, G.A. Molecular cloning of a divinyl ether synthase. Identification as a CYP74 cytochrome P-450. *J. Biol. Chem.* **2001**, *276*, 3620–3627. [[CrossRef](#)]
18. Gorina, S.S.; Toporkova, Y.Y.; Mukhtarova, L.S.; Chechetkin, I.R.; Khairutdinov, B.I.; Gogolev, Y.V.; Grechkin, A.N. Detection and molecular cloning of CYP74Q1 gene: Identification of *Ranunculus acris* leaf divinyl ether synthase. *Biochim. Biophys. Acta* **2014**, *1841*, 1227–1233. [[CrossRef](#)]
19. Gogolev, Y.V.; Gorina, S.S.; Gogoleva, N.E.; Toporkova, Y.Y.; Chechetkin, I.R.; Grechkin, A.N. Green leaf divinyl ether synthase: Gene detection, molecular cloning and identification of a unique CYP74B subfamily member. *Biochim. Biophys. Acta Mol. Cell Biol. Lipids* **2012**, *1821*, 287–294. [[CrossRef](#)]
20. Gorina, S.S.; Toporkova, Y.Y.; Mukhtarova, L.S.; Smirnova, E.O.; Chechetkin, I.R.; Khairutdinov, B.I.; Gogolev, Y.V.; Grechkin, A.N. Oxylipin biosynthesis in spikemoss *Selaginella moellendorffii*: Molecular cloning and identification of divinyl ether synthases CYP74M1 and CYP74M3. *Biochim. Biophys. Acta Mol. Cell Biol. Lipids* **2016**, *1861*, 301–309. [[CrossRef](#)]
21. Yang, Y.; Li, J.; Li, H.; Yang, Y.; Guang, Y.; Zhou, Y. The *bZIP* gene family in watermelon: Genome-wide identification and expression analysis under cold stress and root-knot nematode infection. *PeerJ* **2019**, *7*, e7878. [[CrossRef](#)]
22. Jones, J.T.; Haegeman, A.; Danchin, E.G.; Gaur, H.S.; Helder, J.; Jones, M.G.; Kikuchi, T.; Manzanilla-Lopez, R.; Palomares-Rius, J.E.; Wesemael, W.M.; et al. Top 10 plant-parasitic nematodes in molecular plant pathology. *Mol. Plant Pathol.* **2013**, *14*, 946–961. [[CrossRef](#)] [[PubMed](#)]
23. Yang, Y.X.; Wu, C.; Ahammed, G.J.; Wu, C.; Yang, Z.; Wan, C.; Chen, J. Red light-induced systemic resistance against root-knot nematode is mediated by a coordinated regulation of salicylic acid, jasmonic acid and redox signaling in watermelon. *Front. Plant Sci.* **2018**, *9*, 899. [[CrossRef](#)] [[PubMed](#)]
24. Park, J.H.; Halitschke, R.; Kim, H.B.; Baldwin, I.T.; Feldmann, K.A.; Feyereisen, R. A knock-out mutation in allene oxide synthase results in male sterility and defective wound signal transduction in *Arabidopsis* due to a block in jasmonic acid biosynthesis. *Plant J.* **2002**, *31*, 1–12. [[CrossRef](#)] [[PubMed](#)]
25. Laudert, D.; Pfannschmidt, U.; Lottspeich, F.; Hollander-Czytko, H.; Weiler, E.W. Cloning, molecular and functional characterization of *Arabidopsis thaliana* allene oxide synthase (CYP 74), the first enzyme of the octadecanoid pathway to jasmonates. *Plant Mol. Biol.* **1996**, *31*, 323–335. [[CrossRef](#)] [[PubMed](#)]
26. Kubigsteltig, I.; Laudert, D.; Weiler, E.W. Structure and regulation of the *Arabidopsis thaliana* allene oxide synthase gene. *Planta* **1999**, *208*, 463–471. [[CrossRef](#)] [[PubMed](#)]
27. Song, J.; Zeng, L.; Chen, R.; Wang, Y.; Zhou, Y. In silico identification and expression analysis of superoxide dismutase (SOD) gene family in *Medicago truncatula*. *3 Biotech* **2018**, *8*, 348. [[CrossRef](#)]
28. Madeira, F.; Park, Y.M.; Lee, J.; Buso, N.; Gur, T.; Madhusoodanan, N.; Basutkar, P.; Tivey, A.R.N.; Potter, S.C.; Finn, R.D.; et al. The EMBL-EBI search and sequence analysis tools APIs in 2019. *Nucleic Acids Res.* **2019**, *47*, W636–W641. [[CrossRef](#)]
29. Chen, C.; Chen, H.; He, Y.; Xia, R. TBtools, a Toolkit for Biologists integrating various biological data handling tools with a user-friendly interface. *bioRxiv* **2018**. [[CrossRef](#)]
30. Guo, S.; Zhang, J.; Sun, H.; Salse, J.; Lucas, W.J.; Zhang, H.; Zheng, Y.; Mao, L.; Ren, Y.; Wang, Z.; et al. The draft genome of watermelon (*Citrullus lanatus*) and resequencing of 20 diverse accessions. *Nat. Genet.* **2013**, *45*, 51–58. [[CrossRef](#)]
31. Li, J.; Guang, Y.; Yang, Y.; Zhou, Y. Identification and expression analysis of two *allene oxide cyclase* (AOC) genes in watermelon. *Agriculture* **2019**, *9*, 225. [[CrossRef](#)]
32. Livak, K.J.; Schmittgen, T.D. Analysis of relative gene expression data using real-time quantitative PCR and the $2^{-\Delta\Delta CT}$ method. *Methods* **2001**, *25*, 402–408. [[CrossRef](#)] [[PubMed](#)]

33. La Camera, S.; Gouzerh, G.; Dhondt, S.; Hoffmann, L.; Fritig, B.; Legrand, M.; Heitz, T. Metabolic reprogramming in plant innate immunity: The contributions of phenylpropanoid and oxylipin pathways. *Immunol. Rev.* **2004**, *198*, 267–284. [[CrossRef](#)] [[PubMed](#)]
34. Song, J.; Mo, X.; Yang, H.; Yue, L.; Song, J.; Mo, B. The U-box family genes in *Medicago truncatula*: Key elements in response to salt, cold, and drought stresses. *PLoS ONE* **2017**, *12*, e0182402. [[CrossRef](#)]
35. Matsui, K.; Ujita, C.; Fujimoto, S.; Wilkinson, J.; Hiatt, B.; Knauf, V.; Kajiwarra, T.; Feussner, I. Fatty acid 9- and 13-hydroperoxide lyases from cucumber. *FEBS Lett.* **2000**, *481*, 183–188. [[CrossRef](#)]
36. Shailendar Kumar, M.; Srikanth Chakravarthy, S.; Babu, P.R.; Rao, K.V.; Reddy, V.D. Classification of cytochrome P450s in common bean (*Phaseolus vulgaris* L.). *Plant Syst. Evol.* **2015**, *301*, 211–216. [[CrossRef](#)]
37. Dumin, W.; Rostas, M.; Winefield, C. Identification and functional characterisation of an allene oxide synthase from grapevine (*Vitis vinifera* L. Sauvignon blanc). *Mol. Biol. Rep.* **2018**, *45*, 263–277. [[CrossRef](#)]
38. Zhu, B.Q.; Xu, X.Q.; Wu, Y.W.; Duan, C.Q.; Pan, Q.H. Isolation and characterization of two hydroperoxide lyase genes from grape berries: HPL isogenes in *Vitis vinifera* grapes. *Mol. Biol. Rep.* **2012**, *39*, 7443–7455. [[CrossRef](#)]
39. Yu, J.; Tehrim, S.; Wang, L.; Dossa, K.; Zhang, X.; Ke, T.; Liao, B. Evolutionary history and functional divergence of the cytochrome P450 gene superfamily between *Arabidopsis thaliana* and *Brassica* species uncover effects of whole genome and tandem duplications. *BMC Genomics* **2017**, *18*, 733. [[CrossRef](#)]
40. Tong, X.; Qi, J.; Zhu, X.; Mao, B.; Zeng, L.; Wang, B.; Li, Q.; Zhou, G.; Xu, X.; Lou, Y.; et al. The rice hydroperoxide lyase OsHPL3 functions in defense responses by modulating the oxylipin pathway. *Plant J.* **2012**, *71*, 763–775. [[CrossRef](#)]
41. Chehab, E.W.; Raman, G.; Walley, J.W.; Perea, J.V.; Banu, G.; Theg, S.; Dehesh, K. Rice *HYDROPEROXIDE LYASES* with unique expression patterns generate distinct aldehyde signatures in *Arabidopsis*. *Plant Physiol.* **2006**, *141*, 121–134. [[CrossRef](#)]
42. Wei, K.; Chen, H. Global identification, structural analysis and expression characterization of cytochrome P450 monooxygenase superfamily in rice. *Can. J. Plant Sci.* **2018**, *19*, 35. [[CrossRef](#)]
43. Toporkova, Y.Y.; Gogolev, Y.V.; Mukhtarova, L.S.; Grechkin, A.N. Determinants governing the CYP74 catalysis: Conversion of allene oxide synthase into hydroperoxide lyase by site-directed mutagenesis. *FEBS Lett.* **2008**, *582*, 3423–3428. [[CrossRef](#)]
44. Noordermeer, M.A.; Veldink, G.A.; Vliegthart, J.F. Fatty acid hydroperoxide lyase: A plant cytochrome p450 enzyme involved in wound healing and pest resistance. *ChemBiochem* **2001**, *2*, 494–504. [[CrossRef](#)]
45. Matsui, K. Green leaf volatiles: Hydroperoxide lyase pathway of oxylipin metabolism. *Curr. Opin. Plant Biol.* **2006**, *9*, 274–280. [[CrossRef](#)]
46. Glauser, G.; Grata, E.; Dubugnon, L.; Rudaz, S.; Farmer, E.E.; Wolfender, J.L. Spatial and temporal dynamics of jasmonate synthesis and accumulation in *Arabidopsis* in response to wounding. *J. Biol. Chem.* **2008**, *283*, 16400–16407. [[CrossRef](#)]
47. Gomi, K.; Yamasaki, Y.; Yamamoto, H.; Akimitsu, K. Characterization of a hydroperoxide lyase gene and effect of C₆-volatiles on expression of genes of the oxylipin metabolism in Citrus. *J. Plant Physiol.* **2003**, *160*, 1219–1231. [[CrossRef](#)]
48. Lyons, R.; Manners, J.M.; Kazan, K. Jasmonate biosynthesis and signaling in monocots: A comparative overview. *Plant Cell Rep.* **2013**, *32*, 815–827. [[CrossRef](#)]
49. Per, T.S.; Khan, M.I.R.; Anjum, N.A.; Masood, A.; Hussain, S.J.; Khan, N.A. Jasmonates in plants under abiotic stresses: Crosstalk with other phytohormones matters. *Environ. Exp. Bot.* **2018**, *145*, 104–120. [[CrossRef](#)]
50. Wang, J.; Wu, D.; Wang, Y.; Xie, D. Jasmonate action in plant defense against insects. *J. Exp. Bot.* **2019**, *70*, 3391–3400. [[CrossRef](#)]
51. Kyndt, T.; Nahar, K.; Haecck, A.; Verbeek, R.; Demeestere, K.; Gheysen, G. Interplay between carotenoids, abscisic acid and jasmonate guides the compatible rice-*Meloidogyne graminicola* interaction. *Front. Plant Sci.* **2017**, *8*, 951. [[CrossRef](#)]
52. Nahar, K.; Kyndt, T.; De Vleeschauwer, D.; Hofte, M.; Gheysen, G. The jasmonate pathway is a key player in systemically induced defense against root knot nematodes in rice. *Plant Physiol.* **2011**, *157*, 305–316. [[CrossRef](#)]
53. Martinez-Medina, A.; Fernandez, I.; Lok, G.B.; Pozo, M.J.; Pieterse, C.M.; Van Wees, S.C. Shifting from priming of salicylic acid- to jasmonic acid-regulated defences by *Trichoderma* protects tomato against the root knot nematode *Meloidogyne incognita*. *New Phytol.* **2017**, *213*, 1363–1377. [[CrossRef](#)]

54. Leonetti, P.; Zonno, M.C.; Molinari, S.; Altomare, C. Induction of SA-signaling pathway and ethylene biosynthesis in *Trichoderma harzianum*-treated tomato plants after infection of the root-knot nematode *Meloidogyne incognita*. *Plant Cell Rep.* **2017**, *36*, 621–631. [[CrossRef](#)]
55. Zhao, W.; Zhou, X.; Lei, H.; Fan, J.; Yang, R.; Li, Z.; Hu, C.; Li, M.; Zhao, F.; Wang, S. Transcriptional evidence for cross talk between JA and ET or SA during root-knot nematode invasion in tomato. *Physiol. Genomics* **2018**, *50*, 197–207. [[CrossRef](#)]



© 2019 by the authors. Licensee MDPI, Basel, Switzerland. This article is an open access article distributed under the terms and conditions of the Creative Commons Attribution (CC BY) license (<http://creativecommons.org/licenses/by/4.0/>).